

E-MRS Spring Meeting 2015 Symposium C - Advanced inorganic materials and structures for photovoltaics

## Electronic and structural properties of n-type microcrystalline silicon oxide ( $\mu\text{c-SiO}_x\text{:H}$ ) films for applications in thin film silicon solar cells

V. Smirnov\*, A. Lambertz, and F. Finger

*IEK-5 Photovoltaik, Forschungszentrum Jülich GmbH, D-52425 Jülich, Germany*

### Abstract

The growth of n-type  $\mu\text{c-SiO}_x\text{:H}$  layers in the thickness range of up to 700 nm is investigated. We show that the electrical and structural properties of  $\mu\text{c-SiO}_x\text{:H}$  are thickness dependent but to a weaker extent in comparison with n-type  $\mu\text{c-Si:H}$ .  $\mu\text{c-SiO}_x\text{:H}$  layers with low dark conductivity in the order of  $10^{-11}$  S/cm, measured in the planar direction, can be successfully used as n-layers in amorphous silicon solar cells, resulting in an improved cell performance due to reduced parasitic absorption in the n-type layer. The results suggest anisotropic electrical transport in  $\mu\text{c-SiO}_x\text{:H}$  materials, supported by an observation of elongated crystalline regions in high resolution TEM microscopy.

© 2015 The Authors. Published by Elsevier Ltd. This is an open access article under the CC BY-NC-ND license (<http://creativecommons.org/licenses/by-nc-nd/4.0/>).

Peer-review under responsibility of The European Materials Research Society (E-MRS)

*Keywords:* microcrystalline silicon oxide; growth; thin film solar cells

### 1. Introduction

Due to its wide band gap, adaptable refractive index, and high conductivity doped microcrystalline silicon oxide ( $\mu\text{c-SiO}_x\text{:H}$ ) has been the subject of research as a material for photovoltaic applications [1-12]. As a two phase material,  $\mu\text{c-SiO}_x\text{:H}$  is a mixture of microcrystalline silicon ( $\mu\text{c-Si:H}$ ) and amorphous silicon oxide ( $\text{a-SiO}_x\text{:H}$ ) [2, 4, 5]. The structural and chemical composition of the films can be varied by adjusting the process gas flows. The structural composition (e.g. crystalline volume fraction) or the chemical composition (e.g. the oxygen content) have

\* Corresponding author. Tel.: +49-2461-618725; fax: +49-2461-613735.  
*E-mail address:* v.smirnov@fz-juelich.de

a strong influence on the optical and electrical properties. As a result, the optical band gap ( $E_{04}$ ), refractive index ( $n$ ), crystallinity ( $I_{CRS}$ ) and conductivity of the  $\mu\text{-SiO}_x\text{:H}$  films can be modified over a wide range by adjusting the process gas flows.

Depending on the applications in solar cells,  $\mu\text{-SiO}_x\text{:H}$  layers of adapted composition and thickness are needed. For example, in tandem solar cells, relatively thick  $\mu\text{-SiO}_x\text{:H}$  layers can be placed between sub-cells in order to enable reflection of short wavelength light back to the top amorphous silicon (a-Si:H) sub-cell [4, 8, 10], while in the case of a window or back contact layer, much thinner doped  $\mu\text{-SiO}_x\text{:H}$  layers are used in order to reduce parasitic absorption losses [5, 9, 12]. Therefore it is important to investigate the growth and evolution of the material properties with the thickness of the  $\mu\text{-SiO}_x\text{:H}$  films.

In the present work we investigate the optical, electronic and structural properties of n-type  $\mu\text{-SiO}_x\text{:H}$  films over a wide range of thickness, varied between 20 to 700 nm. Our results indicate that in  $\mu\text{-SiO}_x\text{:H}$  layers the crystallinity slightly increases with layer thickness up to a thickness of around 200 nm and tends to saturate at a level of around 15% for the layers thickness between 200 to 700 nm, while dark conductivity increases from  $10^{-11}$  S/cm up to  $10^{-2}$  S/cm over the entire thickness range. In contrast, n-type  $\mu\text{-Si:H}$  layers (without additional oxygen) show an increase in both crystallinity (up to 70%) and conductivity (up to 5 S/cm) with thickness up to 700 nm. Despite quite low lateral conductivity values for a thickness of around 20 nm as applied in the solar cell (below  $10^{-11}$  S/cm), the applicability of  $\mu\text{-SiO}_x\text{:H}$  layers is demonstrated in a-Si:H single junction solar cells resulting in high initial efficiency of 11.1% and improved spectral response (by around 0.5 mA/cm<sup>2</sup>), relative to a solar cell with a standard n-layer. The results suggest the electrical transport in  $\mu\text{-SiO}_x\text{:H}$  is anisotropic, which is also supported by an observation of elongated crystalline structures in high resolution TEM microscopy images.

## 2. Experimental details

n-type  $\mu\text{-SiO}_x\text{:H}$  layers were deposited by RF (13.56 MHz) plasma enhanced chemical vapour deposition (PECVD) technique at 185°C substrate temperature, at a pressure of 4 mbar and a power of 50 W, using a mixture of silane ( $\text{SiH}_4$ ), hydrogen ( $\text{H}_2$ ), phosphine ( $\text{PH}_3$ ) and carbon dioxide ( $\text{CO}_2$ ) gases. The electrode area and the gap between the electrodes were 167 cm<sup>2</sup> and 2 cm, respectively. The n-type  $\mu\text{-SiO}_x\text{:H}$  films were deposited on glass substrates at a  $\text{SiH}_4$  flow of 1 sccm, a  $\text{H}_2$  flow of 200 sccm, a  $\text{PH}_3$  flow of 0.02 sccm and varied  $\text{CO}_2$  flow. Additional details on the deposition conditions can be found elsewhere [5, 8]. Optical and electrical properties of these layers were investigated by Photothermal Deflection Spectroscopy (PDS) and conductivity measurements, respectively. Conductivity measurements were performed on films equipped with coplanar electrodes 5 mm in length separated by a 0.5 mm gap. The structural properties of  $\mu\text{-SiO}_x\text{:H}$  layers were probed using Raman spectroscopy. The ratio of integrated intensities attributed to crystalline and amorphous regions, Raman intensity ratio  $I_{CRS} = I_c / (I_c + I_a)$  was used as semi-quantitative value of the crystalline volume fraction [5, 8]. TEM microscopy of the FIB (focused ion beam) sectioned cross-section of the layers were carried out using a FEI Tecnai F20 (s)TEM fitted with a Gatan UltraScan 1000P (2kx 2k) CCD camera and equipped with a standard phosphor scintillator using an acceleration voltage of 200kV.

$\mu\text{-SiO}_x\text{:H}$  layers were subsequently used as n-type layers in a-Si:H single junction solar cells. The solar cells were prepared on  $\text{SnO}_2\text{:F}$  substrates (from Asahi company type VU) in a p-i-n deposition sequence with a sputtered aluminum doped zinc oxide/silver ( $\text{ZnO:Al/Ag}$ ) reflecting back contact [13] defining the area (1 cm<sup>2</sup>) of the individual cells. The thickness of the amorphous silicon carbide (a-SiC:H) p-layer and the intrinsic a-Si:H absorber layer was 8 nm and 300 nm, respectively. Additional details on the preparation of the solar cells can be found in refs [8, 12]. Solar cells were characterized by current-voltage ( $J$ - $V$ ) measurements under AM 1.5 illumination using a double source (Class A) sun simulator, and by External Quantum Efficiency ( $EQE$ ) measurements.

### 3. Results

#### 3.1. Material properties

Fig. 1 shows absorption coefficient spectra of  $\mu\text{-SiO}_x\text{:H}$  films (700 nm thick) measured by PDS, as a function of  $\text{CO}_2$  flow varied between 0 and 1.5 sccm. As expected, the optical bandgap  $E_{04}$  increases with an increase in  $\text{CO}_2$  flow and changes between 1.82 to 2.4 eV. The corresponding changes in dark conductivity are shown in Fig. 2 indicating a reduction in dark conductivity  $\sigma_{\text{dark}}$  from several S/cm ( $\text{CO}_2$  flow of 0) down to below  $10^{-11}$  S/cm ( $\text{CO}_2$  flow of 1.5 sccm), in agreement with previous reports [9, 10].

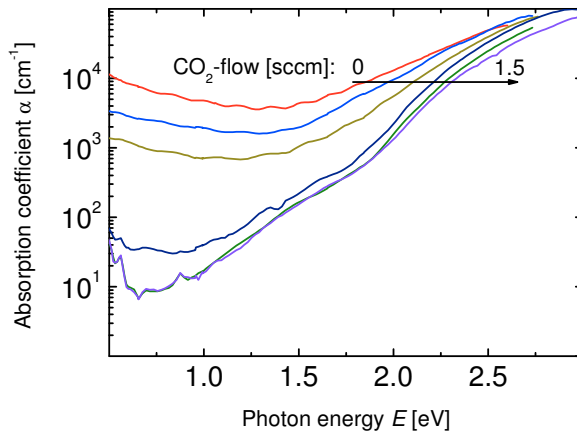


Fig. 1. Absorption coefficient versus the photon energy for n-type  $\mu\text{-SiO}_x\text{:H}$  layers (700 nm thick) with varied  $\text{CO}_2$  flow.

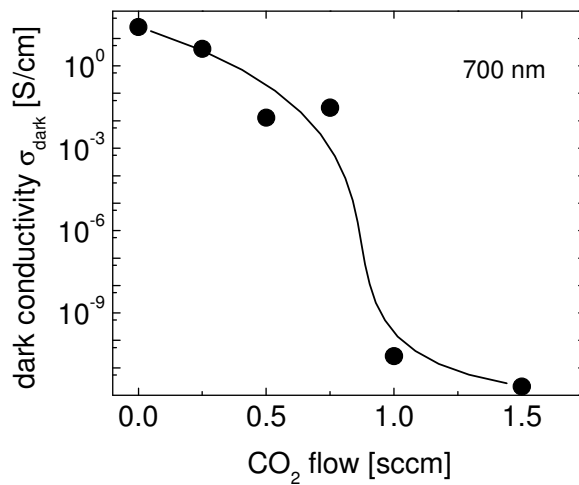


Fig. 2. Dark conductivity ( $\sigma_{\text{dark}}$ ) of  $\mu\text{-SiO}_x\text{:H}$  films prepared at varied  $\text{CO}_2$  flows. The line is to guide the eye.

It was previously reported [5, 8] that an optimal material composition of n-type  $\mu\text{-SiO}_x\text{:H}$  films, used as n-type layers in solar cells, is obtained at  $\text{CO}_2$  flow of 0.75 sccm, and we have subsequently selected this particular flow for more detailed investigation of the evolution in the properties of the  $\mu\text{-SiO}_x\text{:H}$  films with thickness. The effects of thickness on crystallinity  $I_{\text{CRS}}$  and dark conductivity  $\sigma_{\text{dark}}$  are shown in Figs. 3(a) and 3(b) respectively. A qualitatively different behaviour for  $\mu\text{-SiO}_x\text{:H}$  and  $\mu\text{-Si:H}$  films is observed in Fig. 3. It can be seen that in the case of  $\mu\text{-SiO}_x\text{:H}$  layers the crystalline volume fraction ( $I_{\text{CRS}}$ ) increases slightly from around 5% for a layer thickness of 20 nm to up a level of around 15% for the layers thickness between 20 to 700 nm; and the dark conductivity increases from around  $10^{-11}$  S/cm up to  $10^{-2}$  S/cm over the entire thickness range. In contrast, n-type  $\mu\text{-Si:H}$  layers (without additional oxygen) show much high values of both crystallinity and dark conductivity over the thickness range:  $I_{\text{CRS}}$  changes between 50% to 70% and conductivity changes in the range of several S/cm.

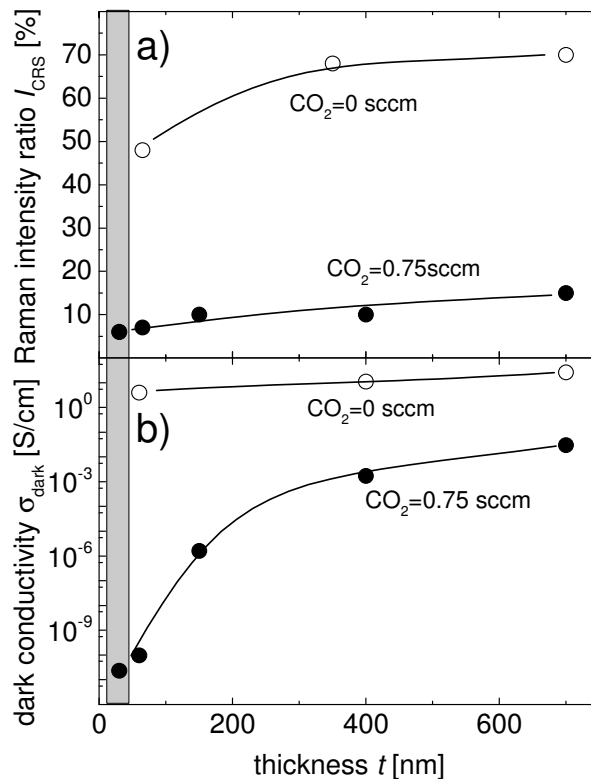


Fig. 3. Raman intensity ratio  $I_{\text{CRS}}$  (a) and dark conductivity  $\sigma_{\text{dark}}$  (b) of n-type  $\mu\text{-SiO}_x\text{:H}$  films of varied thickness ( $\text{CO}_2$  flow of 0.75 sccm, solid cycles). For the purpose of comparison, the properties of n-type  $\mu\text{-Si:H}$  films ( $\text{CO}_2$  flow of 0, open cycles) are shown. The lines are to guide the eye. The layers used in solar cells are shown by grey area.

### 3.2. Solar cell performance

Subsequently, a-Si:H single junction solar cells were prepared with around 20 nm thick  $\mu\text{-SiO}_x\text{:H}$  n-layer layer (indicated by grey area in Fig. 3). Fig. 4 shows  $EQE$  curves of a-Si:H single junction solar cells with  $\mu\text{-SiO}_x\text{:H}$  n-

layer, compared with the solar cells with standard (no oxygen) n-layer. It can be seen that replacing the standard n-layer with an n-type  $\mu\text{-SiO}_x\text{:H}$  layer (solid lines), results in an increased  $EQE$  by around  $0.5 \text{ mA/cm}^2$  up to a value of  $16.9 \text{ mA/cm}^2$ . The gain in  $EQE$  is observed in the wavelength range between 550 nm and 750 nm. This can be a consequence of reduced parasitic absorption [11, 12], which, in turn, could be related to improved transparency of  $\mu\text{-SiO}_x\text{:H}$  layer as shown in Fig. 1. The  $J$ - $V$  characteristics of both types of a-Si:H single junction solar cells show high performance with fill factor values above 70.8% and efficiencies of 11.1% and 11.0% in the case of  $\mu\text{-SiO}_x\text{:H}$  and  $\mu\text{-Si:H}$  n-layers, respectively.

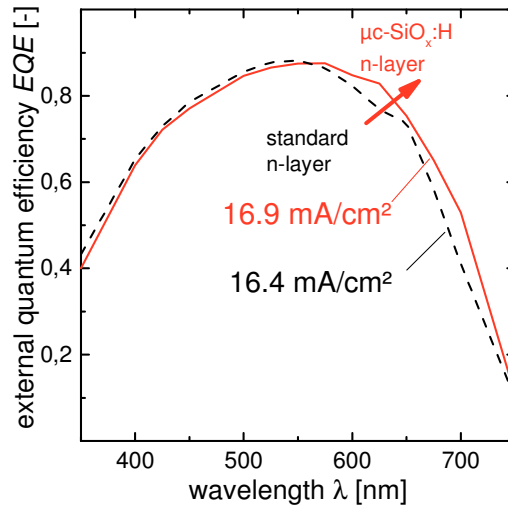


Fig. 4.  $EQE$  curves of a-Si:H solar cells with  $\mu\text{-SiO}_x\text{:H}$  n-layer (red solid line) and standard n-layer (black dashed line). The values next to  $EQE$  curves refer to the calculated current densities.

#### 4. Discussion

The structural evolution of n-type  $\mu\text{-Si:H}$  is evident in Fig. 3, where the crystallinity changes between 48% to 70%. The presence of a nucleation region and an increase in crystallinity with thickness of  $\mu\text{-Si:H}$  layer have been previously reported [14-16]. In contrast to that, the crystallinity of  $\mu\text{-SiO}_x\text{:H}$  changes much weaker with thickness as shown in Fig. 3, where  $I_{\text{CRS}}$  is varied between 6% to 15% over 700 nm range. A general trend in Figs. 3(a) and 3(b) indicates a link between crystallinity ( $I_{\text{CRS}}$ ) and dark conductivity for both types of materials. However, additional oxygen in the layer results in substantially reduced crystallinity and dark conductivity values, which is also supported by the results in Fig. 2 and in agreement with literature [5-9]. The significant differences in crystalline content between  $\mu\text{-SiO}_x\text{:H}$  and  $\mu\text{-Si:H}$  could be responsible for significantly lower dark conductivity values in the case of  $\mu\text{-SiO}_x\text{:H}$ .

Additional information on the growth of  $\mu\text{-SiO}_x\text{:H}$  was obtained with the cross sectional transmission electron microscopy (TEM) measurements. Fig. 5 shows TEM images of  $\mu\text{-SiO}_x\text{:H}$  layers used in the present work. It can be seen in Fig. 5(a) that the microstructure of  $\mu\text{-SiO}_x\text{:H}$  is rather homogeneous with thickness, so that no significant structural evolution is observed. This supports the results of structural studies shown in Fig. 3. High resolution TEM image is shown in Fig. 5(b). It is evident that microstructure of  $\mu\text{-SiO}_x\text{:H}$  contains crystalline structures elongated in the direction of growth, as exemplarily indicated by a yellow cycle in Fig. 5(b). This suggests that the electrical transport in  $\mu\text{-SiO}_x\text{:H}$  could be anisotropic, and therefore the electrical transport in the growth direction, could be enhanced relative to the coplanar conductivity data shown in Fig. 3. Interestingly enough,  $\mu\text{-SiO}_x\text{:H}$  layers with

conductivity values in the order of  $10^{-11}$  S/cm perform well in solar cells with fill factor value of 70.8% and efficiency of 11.1%, which would support the views of anisotropic transport in  $\mu\text{-SiO}_x\text{:H}$ .

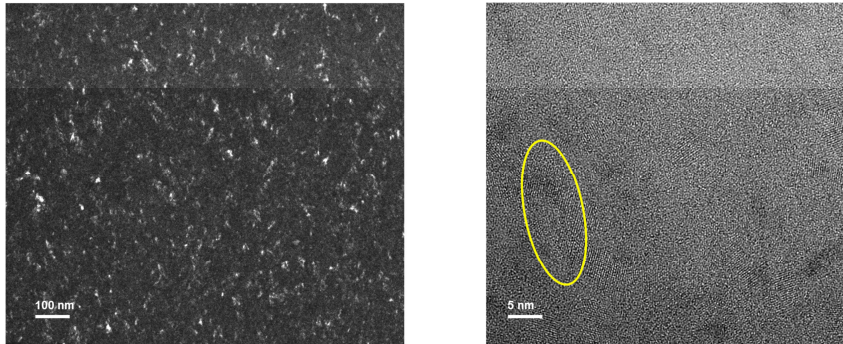


Fig. 5. (a) TEM and (b) HRTEM images of  $\mu\text{-SiO}_x\text{:H}$  layers. The cycle indicates elongated crystalline structures in the direction of growth.

## 5. Conclusions

We have studied the electrical and structural properties of  $\mu\text{-SiO}_x\text{:H}$  layers in the thickness range of up to 700 nm. We have shown that the dark conductivity of  $\mu\text{-SiO}_x\text{:H}$  increases with thickness in the range between  $10^{-11}$  S/cm to  $10^{-2}$  S/cm, while crystallinity increases slightly up to around 15% over a thickness of 700 nm. Despite quite lower dark conductivity values measured in coplanar configuration for the layers around 20 nm thick, these  $\mu\text{-SiO}_x\text{:H}$  layers can be successfully used as n-layers in amorphous silicon solar cells, resulting in an improved cell performance due to reduced parasitic absorption in the n-type layer and efficiency of 11.1%. The results of TEM microscopy indicate the presence of crystalline regions elongated in the direction of growth, supporting the views of anisotropic electrical transport in  $\mu\text{-SiO}_x\text{:H}$  materials.

## Acknowledgements

The authors thank R. Carius, A. Dasgupta, M. Hülsbeck, J. Klomfaß, S. Moll, H. Siekmann and C. Zahren for their contributions to this work. This work was partly supported by the Bundesministerium für Wirtschaft und Energie under contract No. 0325442D.

## References

- [1] D. Das, M. Jana, A. K. Barua, *Sol. Energy Mat. Sol. Cells* **63**, 285 (2000).
- [2] D. Domine, P. Buehlmann, J. Bailat, A. Billet, A. Feltrin, C. Ballif, *Phys. Stat. Sol. (RRL)* **2**, **4**, 163 (2008).
- [3] V. Smirnov, W. Böttler, A. Lambertz, H. Wang, R. Carius, F. Finger, *Phys. Status Solidi C* **7**, 1053 (2010).
- [4] P. Delli Veneri, L.V. Marcaldo, I. Usatii, *Appl. Phys. Lett.* **97** (2), 023512 (2010).
- [5] A. Lambertz, V. Smirnov, T. Merdzhanova, K. Ding, S. Haas, G. Jost, R.E.I. Schropp, F. Finger, and U. Rau, *Sol. Energy Mat. Sol. Cells* **119**, 134 (2013).

- [6] A. Limmanee, S. Kittisontirak, S. Inthisang, T. Krajangsang, J. Sritharathikhun, and K. Sriprapha, *Int. J. Photoenergy*, **2013**, 513284 (2013).
- [7] O. Gabriel, S. Kirner, M. Klingsporn, F. Friedrich, B. Stannowski, R. Schlatmann, *Plasma Proc. Polymers* **12**, 82 (2015).
- [8] V. Smirnov, A. Lambertz, B. Grootoonk, R. Carius, and F. Finger, *J. Non-Cryst. Solids* **358**, 1954 (2012).
- [9] S.-W. Liang, Y.-T. Huang, H.-J. Hsu, C.-H. Hsu and C.-C. Tsai, *Jpn. J. Appl. Phys.* **53** 05FV08 (2014) .
- [10] V. Smirnov, A. Lambertz, S. Tillmanns, and F. Finger, *Can. J. Phys.* **92**, 932 (2014)
- [11] T. Matsui, H. Sai, K. Saito, M. Kondo, *Prog. Photovolt.: Res. Appl.* **21**, 1363 (2013).
- [12] A. Lambertz, F. Finger, R.E.I Schropp, U. Rau, V. Smirnov, *Prog. Photovolt.: Res. Appl.* **23**, 939 (2015).
- [13] W. Böttler, V. Smirnov, J. Hüpkas, and F. Finger, *Phys. Status Solidi A* **209**, 1144 (2012).
- [14] A. Matsuda, S. Yamasaki, K. Nakagawa, H. Okushi, K. Tanaka, S. Iizoma, et al., *Jpn. J. Appl. Phys.* **19** L305 (1980).
- [15] P. Roca i Cabarrocas, N. Layadi, T. Heitz, B. Drévilion, I. Solomon, *Appl. Phys. Lett.* **66**, 3609 (1995)
- [16] J. Kocka, A. Fejfar, H. Stuchlikova, J. Stuchlik, P. Fojtik, T. Mates, B. Rezek, K. Luterova, V. Svrcek, I. Pelant, *Sol. Energy Mater. Sol. Cells*, **78**, 493 (2003)